

Energy Efficient Fair STAR-RIS for Mobile Users

Ashok S. Kumar, Nancy Nayak, Sheetal Kalyani, *Senior Member, IEEE*, and Himal A. Suraweera, *Senior Member, IEEE*

Abstract—In this work, we propose a method to improve the energy efficiency and fairness of simultaneously transmitting and reflecting reconfigurable intelligent surfaces (STAR-RIS) for mobile users, ensuring reduced power consumption while maintaining reliable communication. To achieve this, we introduce a new parameter known as the subsurface assignment variable, which determines the number of STAR-RIS elements allocated to each user. We then formulate a novel optimization problem by concurrently optimizing the phase shifts of the STAR-RIS and subsurface assignment variable. We leverage the deep reinforcement learning (DRL) technique to address this optimization problem. The DRL model predicts the phase shifts of the STAR-RIS and efficiently allocates elements of STAR-RIS to the users. Additionally, we incorporate a penalty term in the DRL model to facilitate intelligent deactivation of STAR-RIS elements when not in use to enhance energy efficiency. Through extensive experiments, we show that the proposed method can achieve fairly high and nearly equal data rates for all users in both the transmission and reflection spaces in an energy-efficient manner.

Index Terms—simultaneously transmitting and reflecting reconfigurable intelligent surfaces, deep reinforcement learning, energy efficiency, user fairness.

I. INTRODUCTION

Conventionally, reconfigurable intelligent surfaces (RISs) enhance the propagation environment by intelligently reflecting incident signals; however, it inherently restricts communication to 180° , leading to potential coverage dead zones [1]. Addressing this limitation, the innovation of simultaneously transmitting and reflecting RIS (STAR-RIS) emerges as a transformative solution [2], [3]. The STAR-RIS can simultaneously reflect and transmit the incident signal, thus providing the coverage to 360° , unlike traditional RIS, which can only reflect [2], [3]. The STAR-RIS can be operated in one of the three practical modes, namely energy splitting (ES), mode switching (MS), and time switching (TS) [2], [3]. The MS mode is preferred in practice among these three protocols due to its ease of hardware implementation. Besides, as reported in [2]–[5], the MS protocol is not restricted by the constraint of transmission-reflection phase correlation, which may cause performance degradation to the ES protocol. Hence, we consider the MS protocol for operating STAR-RIS in this work.

An energy-efficient STAR-RIS is crucial in practical scenarios as it reduces power consumption, minimizes

operational costs, and ensures reliable communication [6], [7]. Energy efficient design of STAR-RIS has been considered in many works to maximize the energy efficiency by jointly optimizing the phase shifts of the STAR-RIS, beamformers at the base station (BS), etc. [7]–[10]. In [7], the authors designed an algorithm to maximize the energy efficiency of a STAR-RIS-assisted multiple-input multiple-output non-orthogonal multiple access (NOMA) system by iteratively optimizing beamforming vectors and phase shifts of STAR-RIS. The work in [8] aims to maximize the energy efficiency of a NOMA-assisted STAR-RIS downlink (DL) network by jointly optimizing beamforming vectors and STAR-RIS coefficients using a deep deterministic policy gradient (DDPG) based algorithm. The paper [9] aims to maximize the energy efficiency of a STAR-RIS-aided full-duplex system by jointly optimizing the transmit power of the BS and the uplink (UL) user and the passive beamforming at the STAR-RIS. In [10], the goal is to maximize the sum rate of all users by jointly optimizing the STAR-RIS's beamforming vectors, the unmanned aerial vehicle's trajectory, and power allocation. However, all the above works [7]–[10] have focused on enhancing energy efficiency by jointly optimizing the phase shifts of the STAR-RIS, beamformers at the base station, and the transmit power of the BS. To the best of our knowledge, none of the previous works optimizes the parameter that tells how many STAR-RIS elements are allotted to a particular user. In this work, we call this parameter as subsurface assignment variable, an indicator that tells how many elements of STAR-RIS are allotted to a specific user.

The first part of our work aims to maximize the fairness and data rates by jointly optimizing the phase shifts of the STAR-RIS and the subsurface assignment variable in the static user scenario. The work in [11] and [12] discusses a multi-user STAR-RIS setup, in which the elements of the STAR-RIS have been partitioned equally into subsurfaces so that the system resources can be utilized more effectively. However, equal partitioning of the STAR-RIS elements can lead to over-utilization or under-utilization of resources. Equal partitioning of the STAR-RIS allots equal elements to all the users, but users closer to the STAR-RIS require fewer elements than those farther away. This leads us to propose unequal partitioning of the STAR-RIS for more efficient resource utilization. Unequal partitioning of STAR-RIS elements allocates more elements to distant users, thereby increasing their data rates. Simultaneously, allocating fewer elements to nearby users can increase the system's energy efficiency. In summary, appropriate unequal partitioning can lead to fair energy efficient STAR-RIS. Our work studies the effect of equal and unequal partitioning, specifically in a multi-user

A. S. Kumar, N. Nayak and S. Kalyani are with the Department of Electrical Engineering, Indian Institute of Technology Madras, Chennai, India (e-mail: {ee22d023@smail, ee17d408@smail, skalyani@ee}.iitm.ac.in).

H. A. Suraweera is with the Department of Electrical and Electronic Engineering, University of Peradeniya, Peradeniya 20400, Sri Lanka (e-mail: himal@eng.pdn.ac.lk).

setup.

The works reported in [13]–[15] use traditional optimization algorithms to solve the non-convex optimization problem of finding the phase shifts of the RIS and beamformers at the base station. The complexity of such algorithms increases with the increasing number of users, increasing the number of STAR-RIS elements, and with unknown communications scenarios [16]. Deep reinforcement learning (DRL) can solve these types of high-dimensional complex problems. Many works explore the advantage of the DRL approach in RIS for predicting the phase shifts of the RIS, active beamformers at the BS [16]–[18], maximizing the weighted sum rate of uplink and downlink users and maximizing the coverage and capacity [19]. Given that the issue with the subsurface assignment variable is inherently a combinatorial problem, we are inspired to employ DRL in our work to predict both the phase shifts of the STAR-RIS and the subsurface assignment variable.

The authors of [20] and [21] consider the scenario of moving users in which they propose an RIS-assisted system that handles users' mobility. In the context of mobile users, equal partitioning falls short due to its inability to adapt to the diverse needs of each user. However, unequal partitioning allows dynamic allocation of the STAR-RIS elements effectively, with varying user demands. Thus, unequal partitioning of STAR-RIS elements is more effective in mobile scenarios than equal partitioning. In mobile users' scenarios, the traditional optimization algorithm faces even greater challenges in optimizing the phase shifts of the RIS and beamformers at the base station as the channel characteristics change over time [17]. Our proposed DRL approach can work well in both static and mobile scenarios.

We also investigate the effect of selective deactivation or shutting down the STAR-RIS elements on our system's performance. We believe that by adopting selective deactivation of elements of STAR-RIS, the overall power consumption of the system can be reduced, and the system can further become more energy efficient. The DRL can decide which elements to shut down by considering user locations, signal strength, and channel conditions. Thus the DRL algorithm helps the STAR-RIS to make real-time decisions about the deactivation of elements to enhance energy efficiency.

The main contributions of our work are summarised as follows:

- In this paper, we propose a fair energy-efficient approach for optimizing STAR-RIS systems in multi-user downlink scenarios. For this, we introduce a new parameter, namely the subsurface assignment variable which determines how many elements of STAR-RIS are allotted to a particular user. This addition brings a new dimension to STAR-RIS, enhancing fairness among users. We then formulate a novel optimization problem by simultaneously considering the phase shift of the STAR-RIS and the subsurface assignment variable. We apply the DRL technique to address this complex optimization problem.
- We explored the possibility of selective deactivation of STAR-RIS elements to increase energy efficiency without

affecting the individual data rates of each user. This can be achieved by incorporating a penalty term in the DRL model. Utilizing the DRL approach, we can intelligently allocate action space and systematically deactivate certain elements of STAR-RIS when not needed, enhancing energy efficiency.

- We analyzed the system's performance in mobile user scenarios also. The DRL allows the STAR-RIS to continuously learn and optimize its configuration in response to users' mobility. The simulation results show that even in the mobile scenario, we can achieve excellent data rates for all the users in transmission and reflection space.

The rest of the paper is organized as follows. Section II presents the system model for the multi-user STAR-RIS system. We detail the proposed fair energy-efficient approach and DRL-based solution in Section III. Section IV provides the simulation results, followed by our conclusions in Section V.

Notations: Scalars are represented in lower-case while vectors and matrices are denoted by bold-face lower-case and bold-face upper-case letters. The transpose and conjugate transpose of a vector or matrix is denoted by $(\cdot)^T$ and $(\cdot)^H$. Also, diag and $\|\cdot\|$ represent the diagonal matrix and Euclidian norm. \mathbb{C} and \mathbb{R} represents complex and real set of numbers.

II. SYSTEM MODEL

Consider the system model as shown in Fig. 1. The direct links between the BS and individual users are assumed to be weak due to blockage. The BS communicates with users through the assistance of a STAR-RIS. The STAR-RIS has N elements arranged in a uniform planar antenna array with dimension $N^h \times N^v$ with a total number of elements $N = N^h N^v$. We consider the DL transmission scenario in a STAR-RIS communication system. The BS has a uniform linear antenna array positioned along the x -axis consisting of M transmit antennas. The surface of STAR-RIS separates the incident signals into two distinct components [3], [22]. One component (reflected signal) is reflected to the same space as the incident signal, i.e., the reflection space, and the other component (transmitted signal) is transmitted to the opposite space as the incident signal, i.e., the transmission space [3]. We have K DL users (DUs) in the reflection space and L DUs in the transmission space such that $K + L < N$. Let x_r and x_t denote the transmit signal of the BS in the reflection space and the transmission space, respectively. Let $p > 0$ denote the transmit power of the BS. We consider the MS protocol for operating STAR-RIS in which all elements of the STAR-RIS are divided into two groups [2], [3]. We have N^t elements operating in the transmission mode and N^r elements operate in the reflection mode [2]. Note that $N^t + N^r = N$. The channel between the BS and STAR-RIS is given by $\mathbf{G} \in \mathbb{C}^{N \times M}$. The channel between STAR-RIS and k -th DU in the reflection space is given by $\mathbf{g}_k^r \in \mathbb{C}^{1 \times N}$ where $k = 1, 2, \dots, K$. Similarly, the channel between STAR-RIS and l -th DU in the transmission space is given by $\mathbf{g}_l^t \in \mathbb{C}^{1 \times N}$ where $l = 1, 2, \dots, L$. Also $\mathbf{h}_k^r \in \mathbb{C}^{1 \times M}$ denotes the channel between

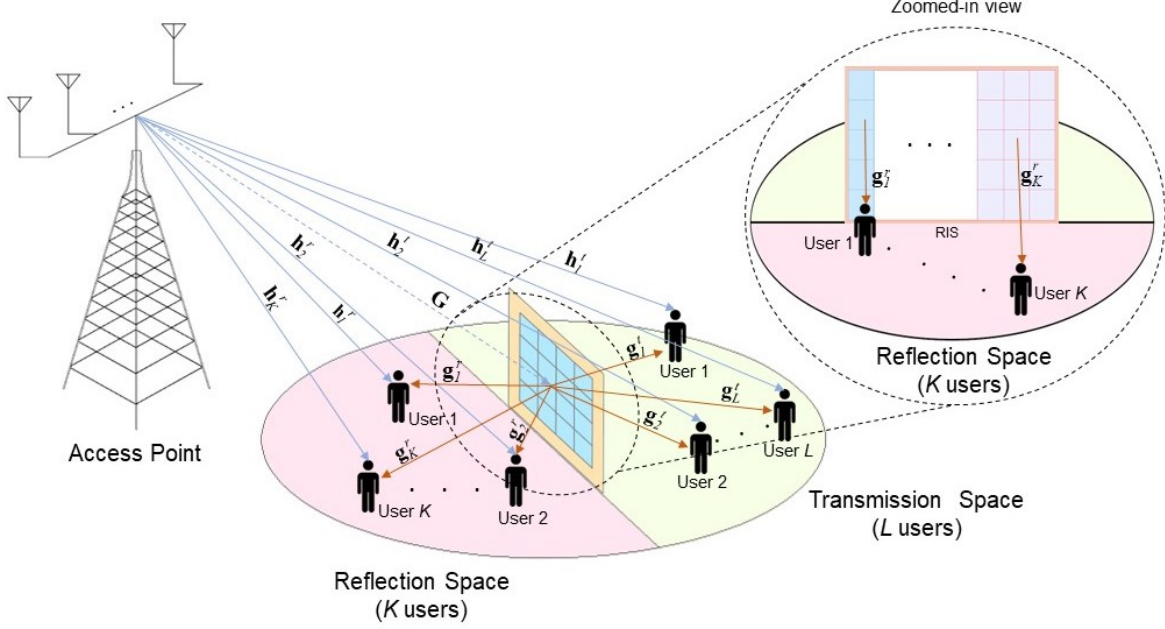


Fig. 1: Proposed system model for multi-user STAR-RIS system with partitioning. We have K users in the reflection space and L users in the transmission space. The zoomed-in view illustrates the partitioning of the N element STAR-RIS. User one being closer, is allocated with fewer number of elements, while user K , being farther, is allocated with more number of elements.

BS and k -th DU in the reflection space and $\mathbf{h}_l^t \in \mathbb{C}^{1 \times M}$ is the channel between BS and l -th DU in the transmission space. The transmission and reflection coefficient matrices of STAR-RIS are given by $\Theta^t, \Theta^r \in \mathbb{C}^{N \times N}$ where,

$$\begin{aligned} \Theta^t &= \text{diag} \left[\sqrt{\beta_1^t} e^{j\theta_1^t}, \dots, \sqrt{\beta_n^t} e^{j\theta_n^t}, \dots, \sqrt{\beta_N^t} e^{j\theta_N^t} \right]^T \\ \Theta^r &= \text{diag} \left[\sqrt{\beta_1^r} e^{j\theta_1^r}, \dots, \sqrt{\beta_n^r} e^{j\theta_n^r}, \dots, \sqrt{\beta_N^r} e^{j\theta_N^r} \right]^T. \end{aligned} \quad (1)$$

Also note that in MS protocol, each element operates in only one mode at a time, either in transmission or reflection mode. Therefore we have $\beta_n^t, \beta_n^r \in \{0, 1\}$, $\beta_n^t + \beta_n^r = 1$ and $\theta_n^t, \theta_n^r \in [0, 2\pi)$ which characterizes the amplitude and phase modifications imposed on the transmitted and reflected signal components, respectively [3]. Assume there is no interference between users in the transmission and reflection space. Let $\mathbf{w} \in \mathbb{C}^{M \times 1}$ be the transmit beamforming vector.

Let $\alpha_{kn}^r \in \{0, 1\}$ be the subsurface (element) assignment variable where $\alpha_{kn}^r = 1$ means that subsurface n is assigned to the k -th user in the reflection space. Also, $\alpha_{ln}^t \in \{0, 1\}$ be the subsurface assignment variable where $\alpha_{ln}^t = 1$ means that subsurface n is assigned to the l -th user in the transmission space. For a specific element n , $\sum_{k=1}^K \alpha_{kn}^r + \sum_{l=1}^L \alpha_{ln}^t \leq 1$, which means that each element of the STAR-RIS should be assigned to at most one user. If an element is shut down, it should not be assigned to any user. However, more than one element can be assigned to one user. So, the subsurface assignment variable will decide whether a particular element of STAR-RIS is allotted to a particular user.

The transmission and reflection coefficients for the k -th user and l -th user in the reflection and transmission space after incorporating subsurface assignment variables are represented as vectors $\mathbf{s}_k^r \in \mathbb{C}^{N \times 1}$ and $\mathbf{s}_l^t \in \mathbb{C}^{N \times 1}$, such that $\mathbf{s}_k^r = [\alpha_{k1}^r \sqrt{\beta_1^r} e^{j\theta_1^r}, \dots, \alpha_{kn}^r \sqrt{\beta_n^r} e^{j\theta_n^r}, \dots, \alpha_{kN}^r \sqrt{\beta_N^r} e^{j\theta_N^r}]^T$ and $\mathbf{s}_l^t = [\alpha_{l1}^t \sqrt{\beta_1^t} e^{j\theta_1^t}, \dots, \alpha_{ln}^t \sqrt{\beta_n^t} e^{j\theta_n^t}, \dots, \alpha_{lN}^t \sqrt{\beta_N^t} e^{j\theta_N^t}]^T$ or equivalently in matrix form as $\tilde{\Theta}_k^r = \text{diag}(\mathbf{s}_k^r)$ and $\tilde{\Theta}_l^t = \text{diag}(\mathbf{s}_l^t)$. We denote

$$\begin{aligned} \boldsymbol{\psi}^r &= [\theta_1^r, \dots, \theta_N^r], \\ \boldsymbol{\psi}^t &= [\theta_1^t, \dots, \theta_N^t] \end{aligned} \quad (2)$$

and $\mathbf{A} = [\mathbf{A}^r, \mathbf{A}^t]^T \in \{0, 1\}^{(K+L) \times N}$, where

$$\begin{aligned} \mathbf{A}^r &= [\alpha_1^r, \alpha_2^r, \dots, \alpha_K^r], \quad \mathbf{A}^t = [\alpha_1^t, \alpha_2^t, \dots, \alpha_L^t] \\ \alpha_k^r &= [\alpha_{k1}^r, \alpha_{k2}^r, \dots, \alpha_{kN}^r]^T, \quad \alpha_l^t = [\alpha_{l1}^t, \alpha_{l2}^t, \dots, \alpha_{lN}^t]^T \end{aligned} \quad (3)$$

The total received signal at the k -th DU in the reflection space is

$$\begin{aligned} y_k &= \mathbf{g}_k^r \tilde{\Theta}_k^r \mathbf{G} \mathbf{w}_k^r x_r \sqrt{p} + \mathbf{h}_k^r \mathbf{w}_k^r x_r \sqrt{p} \\ &+ \sum_{j=1, j \neq k}^K \mathbf{g}_j^r \tilde{\Theta}_j^r \mathbf{G} \mathbf{w}_j^r x_r \sqrt{p} + n, \end{aligned} \quad (4)$$

and the total received signal at the l -th DU in the transmission space is

$$\begin{aligned} y_l &= \mathbf{g}_l^t \tilde{\Theta}_l^t \mathbf{G} \mathbf{w}_l^t x_t \sqrt{p} + \mathbf{h}_l^t \mathbf{w}_l^t x_t \sqrt{p} \\ &+ \sum_{j=1, j \neq l}^L \mathbf{g}_j^t \tilde{\Theta}_j^t \mathbf{G} \mathbf{w}_j^t x_t \sqrt{p} + n, \end{aligned} \quad (5)$$

where n is the additive white Gaussian noise with zero mean and variance σ^2 . Here \mathbf{w}_k^r and \mathbf{w}_l^t represents the beamforming vector for the k -th user and l -th user in the reflection and transmission space, respectively. The objective is to maximize the signal-to-interference-plus-noise ratio (SINR), γ for all the users in both transmission and reflection spaces, which are mathematically expressed as

$$\gamma = \sum_{k=1}^K \gamma_k^r + \sum_{l=1}^L \gamma_l^t = \gamma_r + \gamma_t. \quad (6)$$

Here, γ_k^r denotes the SINR in the reflection space for user k , where

$$\gamma_k^r = \frac{p \|\mathbf{g}_k^r \tilde{\Theta}_k^r \mathbf{G} \mathbf{w}_k^r + \mathbf{h}_k^r \mathbf{w}_k^r\|^2}{\sum_{j=1, j \neq k}^K p \|\mathbf{g}_j^r \tilde{\Theta}_j^r \mathbf{G} \mathbf{w}_k^r\|^2 + \sigma^2}, \quad (7)$$

and γ_l^t represents the SINR in the transmission space for user l , given by

$$\gamma_l^t = \frac{p \|\mathbf{g}_l^t \tilde{\Theta}_l^t \mathbf{G} \mathbf{w}_l^t + \mathbf{h}_l^t \mathbf{w}_l^t\|^2}{\sum_{j=1, j \neq l}^L p \|\mathbf{g}_j^t \tilde{\Theta}_j^t \mathbf{G} \mathbf{w}_l^t\|^2 + \sigma^2}, \quad (8)$$

respectively. The summations extend over all users in the respective spaces. Now, the data rate r_k^r for k -th user in the reflection space can be expressed as

$$r_k^r = \log_2(1 + \gamma_k^r), \quad (9)$$

and the data rate r_l^t for l -th user in the transmission space is

$$r_l^t = \log_2(1 + \gamma_l^t). \quad (10)$$

In this work, we design the transmit beamformers using maximum ratio transmission (MRT) processing [16]. The MRT beamforming is designed to enhance the SINR. The beamforming vector \mathbf{w}_k^r for the k -th user in the reflection space is

$$\mathbf{w}_k^r = \frac{(\mathbf{g}_k^r \tilde{\Theta}_k^r \mathbf{G} + \mathbf{h}_k^r)^H}{\|\mathbf{g}_k^r \tilde{\Theta}_k^r \mathbf{G}\|^2}, \quad (11)$$

and the corresponding beamforming vector \mathbf{w}_l^t for the l -th user in the transmission space is

$$\mathbf{w}_l^t = \frac{(\mathbf{g}_l^t \tilde{\Theta}_l^t \mathbf{G} + \mathbf{h}_l^t)^H}{\|\mathbf{g}_l^t \tilde{\Theta}_l^t \mathbf{G}\|^2}. \quad (12)$$

Our objective is to focus on optimizing the phase shift of the STAR-RIS and the subsurface assignment variable for energy efficiency, which are critical for achieving fair data rates for users in both static and dynamic environments. It is also feasible to optimize the beamformers, but that is outside the scope of our work.

The channels between the STAR-RIS and BS, STAR-RIS and users, and between the BS and users are modeled according to Rician fading [23], [24]. In the case of static users, we consider a Rician channel, which remains constant over time. We consider the time-varying channel model for mobile users, which comprises two primary paths. The first path is the direct link between the BS and users. The second path involves the cascaded channel between the BS and STAR-RIS and STAR-RIS and the users. The channel between

the BS and k -th user in the reflection space can be modeled as [25]

$$\mathbf{h}_k^r(t) = B_k^b(t) \left(\sqrt{\frac{\kappa_d^L}{\kappa_d^L + 1}} \mathbf{h}_k^L(t) + \sqrt{\frac{1}{\kappa_d^{\text{NL}} + 1}} \mathbf{h}_k^{\text{NL}}(t) \right). \quad (13)$$

Here $\mathbf{h}_k^L(t)$ and $\mathbf{h}_k^{\text{NL}}(t)$ represents the line-of-sight (LoS) and non LoS component of $\mathbf{h}_k^r(t)$. The LoS component $\mathbf{h}_k^L(t)$ is given by $\mathbf{h}_k^L(t) = \exp(-j2\pi(f_c + f_k(t))\tau_k(t))$, where $f_k(t)$ is the Doppler frequency shift for $\mathbf{h}_k^r(t)$ and f_c is the carrier frequency. The non-LoS component, $\mathbf{h}_k^{\text{NL}}(t)$ can be modeled as a complex Gaussian distribution $\mathcal{CN}(0, 1)$ for a given time t [25]. The channel gain of the direct link of the k -th user is given by $B_k^b(t) = \frac{\lambda}{4\pi(d_k(t))^{\zeta/2}}$. Here $d_k(t) = \|D_k(t) - D_{\text{BS}}\|$, λ is the carrier wavelength and ζ represents the path loss exponent. Note that $D_k(t)$ represents the location vector of the k -th user at time instant t , and D_{BS} denotes the location vector of the BS. The delay of the direct link of the k -th user can be calculated as $\tau_k(t) = \frac{d_k(t)}{c}$, where c is the speed of light. Let κ_d^L and κ_d^{NL} be respectively the Rician factors for $h_k^L(t)$ and $h_k^{\text{NL}}(t)$. The channel between STAR-RIS and k -th user in the reflection space can be modeled as [25],

$$\mathbf{g}_k^r(t) = B_k^r(t) \left(\sqrt{\frac{\xi_d^L}{\xi_d^L + 1}} \mathbf{g}_k^L(t) + \sqrt{\frac{1}{\xi_d^{\text{NL}} + 1}} \mathbf{g}_k^{\text{NL}}(t) \right). \quad (14)$$

Similarly, the channel between BS and STAR-RIS can be modeled as

$$G(t) = B_b^r \left(\sqrt{\frac{\rho_d^L}{\rho_d^L + 1}} G^L + \sqrt{\frac{1}{\rho_d^{\text{NL}} + 1}} G^{\text{NL}}(t) \right). \quad (15)$$

The channel gain of the STAR-RIS to k -th user links and BS to STAR-RIS are given by $B_k^r(t) = \frac{\lambda}{4\pi(d_k^r(t))^{\zeta/2}}$ and $B_b^r = \frac{\lambda}{4\pi(d_b^r)^{\zeta/2}}$, respectively [25]. Here $d_k^r(t) = \|D_k(t) - D_R\|$ and $d_b^r = \|D_R - D_{\text{BS}}\|$. Also, D_R denotes the location vector of the STAR-RIS. The delay of the cascaded link is $\tau_c(t) = \tau_b^r + \tau_k^r(t) = \frac{d_b^r}{c} + \frac{d_k^r(t)}{c}$. The LoS component $g_k^L(t)$ is given by $g_k^L(t) = \exp(-j2\pi(f_c + f_k^r(t))\tau_k^r(t))$. ξ_d^L and ξ_d^{NL} respectively denote Rician factors of the LoS and non-LoS components of $g_k^r(t)$ and $f_k^r(t)$ represents the Doppler shift for $g_k^r(t)$. Similarly, G^L is given by $G^L = \exp(-j2\pi f_c \tau_b^r)$. Also, ρ_d^L and ρ_d^{NL} are Rician factors of the LoS and non-LoS components of $G(t)$, respectively. Also, note that $g_k^{\text{NL}}(t) \sim \mathcal{CN}(0, 1)$, and $G^{\text{NL}}(t) \sim \mathcal{CN}(0, 1)$. Note that G^L is not a function of time. The value of G^L is taken as one. Similar expressions can be derived for users within the transmission space as well.

III. PROPOSED FAIR ENERGY EFFICIENT APPROACH AND DEEP REINFORCEMENT LEARNING BASED SOLUTION

We aim to maximize the overall SINR so that all the users are served well. We try to find the optimal subsurface assignment and the corresponding optimal phase shift. For this, we formulate the following optimization problem and later solve it using the DRL approach. The optimization problem is framed as follows:

$$\begin{aligned}
\mathcal{P}_1 : \quad & \max_{\psi^r, \psi^t, \mathbf{A}} \sum_{k=1}^K \gamma_k^r + \sum_{l=1}^L \gamma_l^t \\
\text{s.t.} \quad & 0 \leq \angle(\tilde{\Theta}_k^r) \leq 2\pi \\
& 0 \leq \angle(\tilde{\Theta}_j^t) \leq 2\pi \\
& \sum_{n=1}^N \alpha_{kn}^r \geq 1 \quad \forall k \in 1, 2, \dots, K \\
& \sum_{n=1}^N \alpha_{ln}^t \geq 1 \quad \forall l \in 1, 2, \dots, L
\end{aligned} \tag{16}$$

Recall α_{kn}^r is the n -th subsurface assignment variable corresponding to k -th user in the reflection space, and α_{ln}^t is the n -th subsurface assignment variable corresponding to l -th user in the reflection space. It should be noted that $\sum_{n=1}^N \alpha_{kn}^r \geq 1$, which indicates that at least one subsurface must be assigned to the k -th user in the reflection space. Similarly, $\sum_{n=1}^N \alpha_{ln}^t \geq 1$ indicates that at least one subsurface must be assigned to l -th user in the transmission space. We investigate the scenarios of static and dynamic users in the STAR-RIS-assisted system. For both cases, the optimization problem is the same.

The proposed optimization problem \mathcal{P}_1 in (16) maximizes the SINR for all the users in both transmission and reflection spaces. Further, we propose a method to enhance energy efficiency by selective deactivation of the STAR-RIS elements. We discuss this energy efficiency technique later in (18). In both cases, the optimization objective is non-convex with integer constraints on the subsurface assignment variable. Also, the optimization problem lacks closed-form expression due to its high dimensional parameters. Solving this type of optimization problem with numerical methods is challenging. Notably, previous works [26]–[28] have addressed this type of non-convex problem with integer constraints and solved by using DRL because DRL can handle high-dimensional and combinatorial optimization problems more effectively. Motivated by this, we also employ DRL based approach for solving the proposed optimization problem.

We formulate the problem of estimating the phase shift of the STAR-RIS and subsurface assignment variable as a Markov decision process (MDP). The MDP has a state space (\mathcal{S}), an action space (\mathcal{A}), an initial state distribution $p(\mathbf{s}^{\{1\}})$, a stationary state transition distribution $p(\mathbf{s}^{\{t+1\}})$ adhering to the Markov property [29], [30]. The learning process is assessed by the reward function $r^{\{t\}} : \mathcal{S} \times \mathcal{A} \rightarrow \mathbb{R}$, which evaluates the effectiveness of state-action pairs [30]. Fig. 2. shows the MDP formulation in the STAR-RIS system with DRL based learning agent. Here the learning agent takes the state $\mathbf{s}^{\{t\}}$ and reward $r^{\{t\}}$ as input. It then generates the action $\mathbf{a}^{\{t\}}$, which determines the phase shift of the STAR-RIS and the subsurface assignment variable. The superscript t indicates the values at the time step t . The predicted action for time step t can be expressed as $\mathbf{a}^{\{t\}} = [\psi^{r\{t\}}, \psi^{t\{t\}}, \mathbf{A}^{\{t\}}]$ (refer to (2) and (3)). The actions predicted by the model guide the transmission of signals from the BS at time step t . The resulting SINR at the users in both transmission ($\gamma_t^{\{t\}}$) and reflection spaces ($\gamma_r^{\{t\}}$) indicate the effectiveness

of the chosen actions. These SINRs become part of the observed environment and contribute to the state representation $\mathbf{s}^{\{t+1\}}$ for the next iteration of the learning agent. We have $\mathbf{s}^{\{t+1\}} = [\gamma_t^{\{t\}}, \gamma_r^{\{t\}}, \psi^{r\{t\}}, \psi^{t\{t\}}, \mathbf{A}^{\{t\}}]$ (refer to (2), (3), (7) and (8) respectively). The reward is calculated as the average data rate of all users across the transmission and reflection spaces. The data rate at time step t for user k in the reflection space is given by $r_k^{r\{t\}} = \log_2(1 + \gamma_k^{r\{t\}})$. Similarly, the data rate at time step t for user l in the transmission is given by $r_l^{t\{t\}} = \log_2(1 + \gamma_l^{t\{t\}})$. The total reward at time step t can be expressed as

$$r^{\{t\}} = \frac{1}{K+L} \left(\sum_{k=1}^K r_k^{r\{t\}} + \sum_{l=1}^L r_l^{t\{t\}} \right). \tag{17}$$

In our work, we also investigate the possibility of selective deactivation of the elements of the STAR-RIS by using a DRL-based solution. In that case, we propose a modified reward function, namely

$$r^{\{t\}} = \frac{1}{K+L} \left(\sum_{k=1}^K r_k^{r\{t\}} + \sum_{l=1}^L r_l^{t\{t\}} \right) + \frac{\mu}{\sum_{i=1}^{N^t} \sum_{j=1}^{N^r} \mathbf{A}_{ij}^{\{t\}}}. \tag{18}$$

The first term represents the average data rate for all users at time step t . The second term is a regularization term that includes the regularization parameter μ that adds a penalty based on the total number of active elements in the system. By adding a penalty term to the reward function, we can enhance the energy efficiency of the system by limiting the use of excessive active elements. The penalty term balances the trade-off between achieving fair data rates among users and penalizes the presence of redundant excess active elements allocated to a particular user. Note now with $r^{\{t\}}$, as in (18), we also have additional integer constraints while solving for \mathcal{P}_1 . The goal of the RL agent is to learn a policy, denoted as $\pi : \mathcal{S} \rightarrow \mathcal{A}$, to maximize the expected cumulative return, $\mathbb{E}[r^{\{t\}}(\eta)|\pi]$, by considering the discounted rewards obtained at each time step t . Here η denotes the discounting factor ($\eta \in [0, 1]$). The agent evaluates the value of the state using value functions and computes the value of the action by using the Q function [30].

The DRL agent is trained using an actor-critic method named DDPG. The DDPG algorithm simultaneously learns the Q function and policy and it uses policy data and the Bellman equation to learn the Q function which is then utilized to optimize the policy [31]. It contains four neural networks, namely actor network, critic network, target actor network, and target critic network [31]. The actor network Π , which is parameterized by θ^a takes the current state $\mathbf{s}^{\{t\}}$ of the environment as input and produces the corresponding action $\mathbf{a}^{\{t\}}$ as its output [16]. On the other hand, the critic network Δ , which is parameterized by θ^c takes both the state and action as input and produces an output value that evaluates the effectiveness of the current policy [31]. Two target networks were used to make learning more stable. The target actor network is parameterized by $\tilde{\theta}^a$, and the target critic network is parameterized by $\tilde{\theta}^c$. The environment gives the reward $r^{\{t\}}$ after each action. This tells about the effectiveness of the

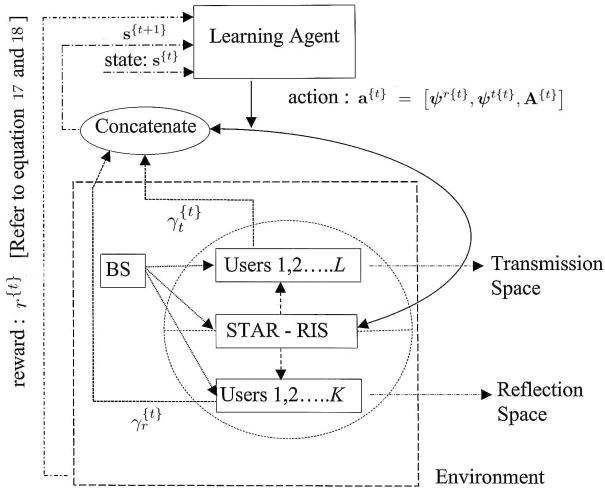


Fig. 2: MDP formulation in STAR-RIS system with DRL based learning agent.

action. At each training time step t , the current state ($\mathbf{s}^{\{i\}}$), the executed action ($\mathbf{a}^{\{i\}}$), the obtained reward ($r^{\{i\}}$), and the subsequent state ($\mathbf{s}^{\{i+1\}}$) are recorded as an experience ($\mathbf{s}^{\{i\}}, \mathbf{a}^{\{i\}}, r^{\{i\}}, \mathbf{s}^{\{i+1\}}$) in buffer B [31]. To train the neural networks, \tilde{N} samples are taken from the B . This is used to compute the gradients. The loss function mean squared Bellman error is given by

$$\hat{L} = \frac{1}{\tilde{N}} \sum_{i=1}^{\tilde{N}} \left(y^{\{i\}} - \Delta \left(\mathbf{s}^{\{i\}}, \mathbf{a}^{\{i\}} \mid \theta^c \right) \right)^2, \quad (19)$$

where $\Delta(\mathbf{s}^{\{i\}}, \mathbf{a}^{\{i\}} \mid \theta^c)$ represents the predicted output value of the critic network and $y^{\{i\}}$ denotes the predicted return which is given by

$$y^{\{i\}} = r^{\{i\}} + \eta \Delta \left(\mathbf{s}^{\{i+1\}}, \Pi(\mathbf{s}^{\{i+1\}} \mid \tilde{\theta}^a) \mid \tilde{\theta}^c \right), \quad (20)$$

[31]. The parameters of the critic network are updated according to $\theta^c \leftarrow \theta^c - \eta_c \nabla_{\theta^c} L$, where $\eta_c \ll 1$ denotes the step size for the stochastic update. For the actor-network, the update is according to $\theta^a \leftarrow \theta^a + \eta_a \frac{1}{\tilde{N}} \sum_{i=1}^{\tilde{N}} \left(\nabla_{\theta^a} \Pi(\mathbf{s}) \nabla_a \Delta(\mathbf{s}, \mathbf{a}) \mid_{\mathbf{a}=\Pi(\mathbf{s})} \right)$ where $\eta_a \ll 1$ denotes the step size for the stochastic update. Also, the DDPG agents update their target actor and critic parameters using $\tilde{\theta}^a \leftarrow \lambda \theta^a + (1-\lambda)\tilde{\theta}^a$ and $\tilde{\theta}^c \leftarrow \lambda \theta^c + (1-\lambda)\tilde{\theta}^c$ with $\lambda \ll 1$.

Our work addresses a pseudo-discrete action space where the STAR-RIS phase shift is continuous while the subsurface assignment variable is discrete. Deep Q-Networks, which are suitable for handling discrete action spaces, cannot be directly applied to handle a mixed action space like ours [32]. We use a two-part neural network to address the huge action space involving STAR-RIS phase shift, and subsurface assignment variable. The first part, a feed-forward feature extractor (FE) with \tilde{L} linear layers using ReLU as an activation function and layer normalization, feeds its output to the second part, comprising two sub-networks (SN) that determines the phase shifts and subsurface assignment variable [16]. At time step t , the input to the FE is the state $\mathbf{u}_0 = \mathbf{s}^{\{t\}}$.

Each layer in FE is represented by weights $\mathbf{W}_l \in \mathbb{R}^{d_o^l \times d_i^l}$ and biases $\mathbf{b}_l \in \mathbb{R}^{d_o^l}$, where $l = 1, 2, \dots, \tilde{L}$, denotes the layer index and d_o^l is the output dimension, and d_i^l is the input dimension. The output of FE ($\mathbf{u}_l \in \mathbb{R}^{d_o^l}$) is given by $\mathbf{r}_l = \text{ReLU}(\mathbf{W}_l \mathbf{u}_{l-1} + \mathbf{b}_l)$. The final output of the FE \mathbf{u}_L is then fed to the SNs. The first SN predicts the STAR-RIS phases with parameters $\mathbf{W}_p \in \mathbb{R}^{N \times d_o^L}$ and biases $\mathbf{b}_p \in \mathbb{R}^N$. We have $\mathbf{a}_p = \tanh(\mathbf{W}_p \mathbf{u}_L + \mathbf{b}_p)$. Similarly, the second SN predicts the subsurface assignment variable with parameters $\mathbf{W}_A \in \mathbb{R}^{N \times d_o^L}$ and biases $\mathbf{b}_A \in \mathbb{R}^N$. We have $\mathbf{a}_A = \tanh(\mathbf{W}_A \mathbf{u}_L + \mathbf{b}_A)$. It should be noted that in the DRL algorithm, the initially predicted continuous actions follow a Gaussian distribution with mean zero and unit standard deviation [16]. This makes it a challenge for the DRL to predict actions that lack symmetry. So, it is essential to normalize the actions using the hyperbolic tangent (tanh) activation function at the final layer of each SN. This normalization ensures that the actions are symmetric and confined within the range of $[-1, +1]$. Later, we adjust the output according to domain-specific knowledge of STAR-RIS phases and subsurface assignment variables through shifting and scaling.

IV. RESULTS AND DISCUSSION

In this section, we will investigate the performance of the proposed method with numerical results. The placement of STAR-RIS, BS, and users are closely aligned with [33], [34] in the three-dimensional Cartesian coordinate system. We have considered different locations for the users relative to STAR-RIS to have varying channel conditions. We assume that the BS is located at $(0, 0, 0)$, and the STAR-RIS is located at $(48, 20, 3)$. We consider three users in the reflection space and three users in the transmission space. The placement of users concerning the STAR-RIS significantly impacts their data rates. Users 1, 2, and 3 are located in the transmission space. Users 4, 5, and 6 are located in the reflection space. For the transmission space, the location of User 2 is closer to the STAR-RIS. User 3 is far away from the STAR-RIS. The location of User 1 is in between Users 2 and 3. Similarly, for the reflection space, User 5 is closer to the STAR-RIS, and User 6 is far from the STAR-RIS. Here, the location of User 4 is between Users 5 and 6. The channels between the BS to STAR-RIS, STAR-RIS to users, and BS to users are modeled as Rician channels as mentioned in Section II. The values of the Rician factors are taken as 10 [24]. The bandwidth where the system operates is 100MHz [35], and the noise power density is -174dBm/Hz [36]. The carrier frequency f_c is taken as 3.5GHz. The path loss between two points with distance \bar{d} is modeled as [37],

$$PL(f_c, \bar{d})_{dB} = -20 \log_{10}(4\pi f_c / c) - 10\zeta \log_{10}(\bar{d}/D_0), \quad (21)$$

where $D_0 = 1\text{m}$, ζ is the path loss exponent. The path loss components in the channel from BS to STAR-RIS and from the STAR-RIS to the users are $\zeta = 2.2$ [38]. The same in the channel from the BS to the users are $\zeta = 3.45$ [38]. We consider the value of discounting factor η as 0.6 for the DRL agent. The buffer size is taken as 10000. The learning rate for the actor and critic network is taken as 0.0001 and

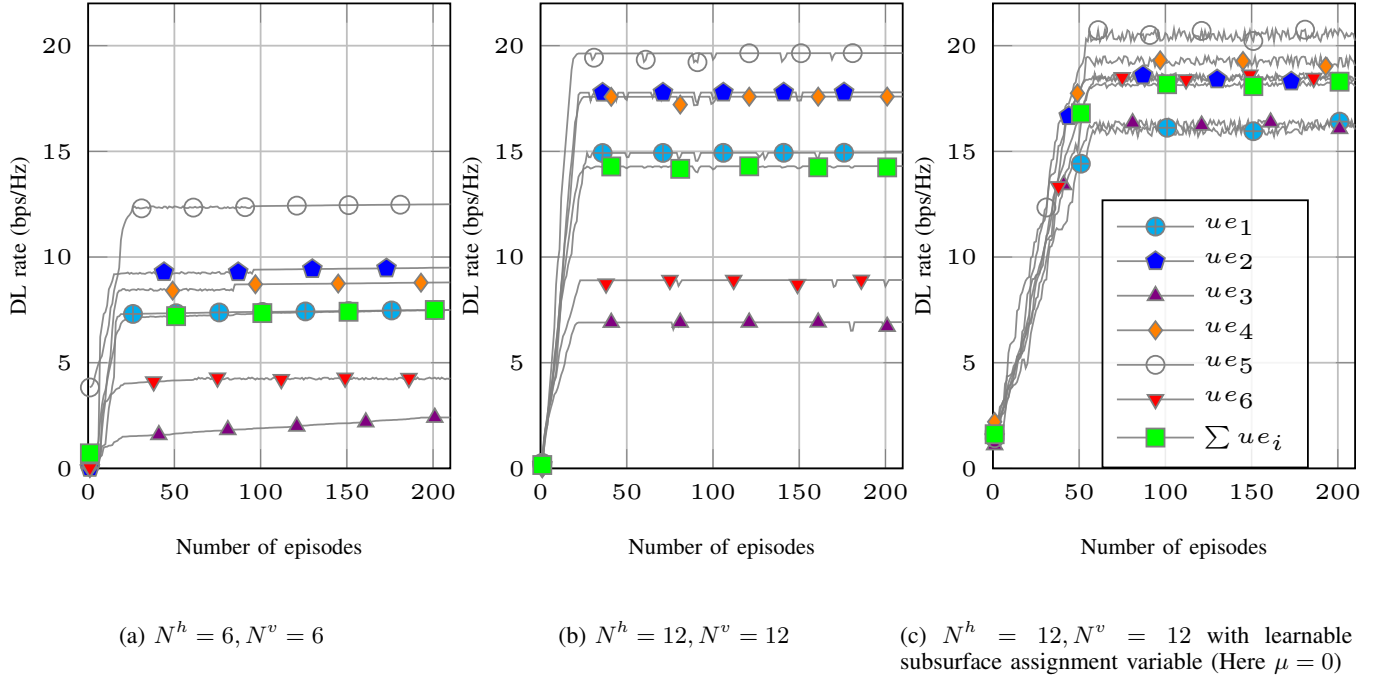


Fig. 3: The effect of increasing the number of STAR-RIS elements is shown in (a) and (b) where the elements are equally partitioned between the users irrespective of their location and channel condition. The DL rate for k -th user is represented with ue_k . The overall DL rate ($\sum ue_i$) improves when STAR-RIS elements are partitioned based on the learnable subsurface assignment variable as shown in (c). The legends are shared across the subfigures.

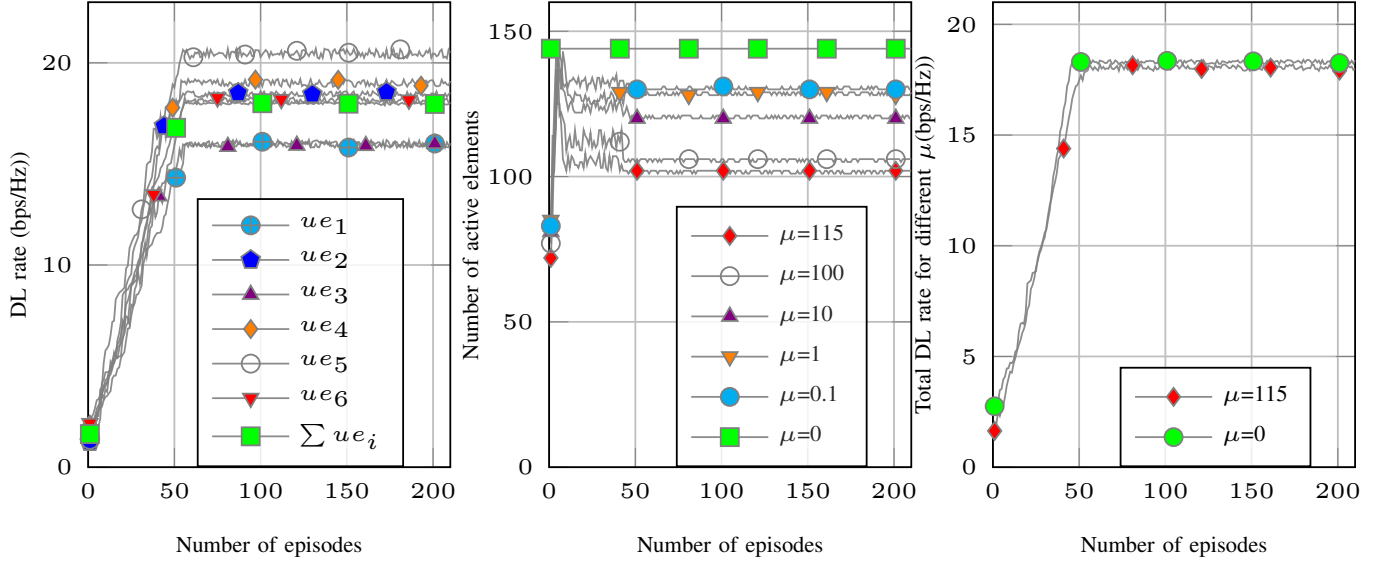
0.001 respectively. The experiment is conducted for an initial 210 episode with each episode consisting of 1000 time steps. The results are averaged over four independent runs. The experiments are performed using an NVIDIA GeForce RTX 2080 Ti GPU. The benchmark metric is DL rate to evaluate the performance and is measured in bits per second per Hertz (bps/Hz).

A. Impact of our proposed approach on energy efficiency and fairness

We first investigate the effect of equal partitioning of STAR-RIS elements in the static user scenario. Fig. 3a considers the scenario of $N^h = N^v = 6$ elements with equal partitioning to all the six users. Here, six elements are allotted to each of the six users. We can see that the DL data rate (in bps/Hz) of users located near STAR-RIS (User five and User two) is high. It can also be observed that users located far from STAR-RIS (User three and User six) have a low DL data rate. The conclusion is that equal partitioning leads to poor data rates for users located far from the STAR-RIS and, hence, is not fair. We will now examine the effect of increasing the STAR-RIS elements when using equal partitioning. Fig. 3b considers the same scenario with increasing the number of STAR-RIS elements to $N^h = N^v = 12$. In this setup, we consider 24 elements allotted to each of the users in the transmission and reflection space. While the overall DL data rate of the entire system increases, the DL data rates of distant users also increase at a much higher rate. So, this scale-up effect indicates that increasing the number of STAR-RIS elements increases the

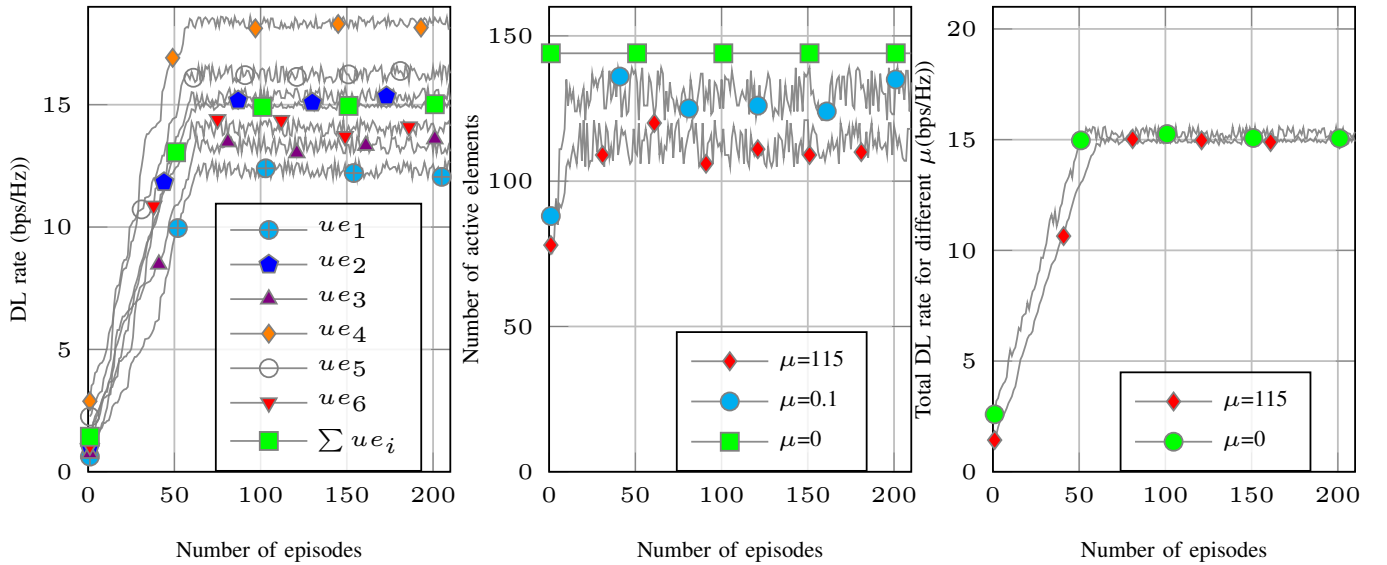
overall data rate and improves communication performance for all users.

Now, we will explore the scenarios where, instead of equal partitions, the subsurface assignment variable (recall (3)) can be learned through DRL for the static user scenario. Here, we consider the scenario of $N^h = N^v = 12$ STAR-RIS elements. The methodology involves training a DDPG algorithm to predict the number of STAR-RIS elements allocated to each user and predicting the phase. We introduce a modified reward function (recall (18)) that combines the average data rate of all users with a regularization parameter μ , which penalizes the presence of active RIS elements. Firstly, we will analyze the case when $\mu = 0$ (17). It can be observed that the DRL model proves advantageous in predicting the sub-surface assignment matrix, optimizing the allocation of STAR-RIS elements to users. This predictive capability leads to improvements in overall data rates, mainly benefiting the users who are spatially distant from the STAR-RIS. As compared to equal partitioning, we can see that the overall data rate increases by an amount of 21% (Fig. 3c). Also, we can see that User three and User six are the ones who benefited the most. An additional observation made from the results is that Users 1, 2, and 5 exhibit nearly comparable data rates as that of the scenario involving equal partitioning of elements, i.e. our proposed DRL-based model is able to achieve fairness among users without compromising on the data rates. This also indicates that achieving the same data rate does not necessarily require the utilization of all elements of STAR-RIS. Thus a subset of the STAR-RIS elements is sufficient to achieve comparable performance. In other words, we can shut down or deactivate some elements



(a) $N^h = N^v = 12$ with $\mu = 115$ (b) $N^h = N^v = 12$ with varying μ values (c) $N^h = N^v = 12$ (μ values = 0 and 115)

Fig. 4: The effect of shutting down the elements of STAR-RIS in a static user scenario: (a) Data rate plot (better visible in colour) (b) Number of active elements for different μ values vs. number of episodes, and (c) Total data rate vs. number of episodes for different μ values. Notably, the total data rate remains nearly constant for μ values of 0 and 115.



(a) $N^h = N^v = 12$ with $\mu = 115$ (b) $N^h = N^v = 12$ with varying μ values (c) $N^h = N^v = 12$ (μ values = 0 and 115)

Fig. 5: The effect of shutting down the elements of STAR-RIS in a mobile user scenario: (a) Data rate plot (better visible in colour) (b) Number of active elements for different μ values vs. number of episodes, and (c) Total data rate vs. number of episodes for different μ values. Even in dynamic scenarios, the total data rate remains similar for μ values of 0 and 115. The observed fluctuations in the graphs are due to the dynamic nature of the scenario, where phase-shift and subsurface assignment variable of the star-RIS are continuously optimized using DRL.

and still achieve high data rates for all users. This observation underscores the potential for optimizing energy consumption by selectively shutting down certain STAR-RIS elements without compromising communication performance.

Now, we will investigate the effect of shutting down the elements of STAR-RIS in a static user scenario. For this, we consider the case of $N^h = N^v = 12$ STAR-RIS elements. Fig. 4a shows the data rate plot by strategically shutting down some of the elements in a STAR-RIS. Here, the value of μ is taken as 115 (recall (18)). A comparatively higher value of μ forces the DRL agent to selectively deactivate the excess STAR-RIS elements. We can achieve almost the same data rate as that of the scenario that we discussed in Fig 3c. The DRL agent can decide which elements to shut down when the total number of elements to a particular user is high while ensuring desired data rates. Recall that by introducing a penalty term into the reward function, the DRL agent can learn the optimal policy and enable the STAR-RIS to make informed decisions about the selective deactivation of elements in real-time, thus achieving energy efficiency without sacrificing overall system performance. Fig. 4b shows the plot between the total number of active elements for different μ values and the number of episodes. As the value of μ increases, we can observe that there is a decrease in the total number of active elements serving the users in transmission and reflection space. For the baseline case, with μ equals zero, all the elements of STAR-RIS are active. For μ values ranging from 0.1 to 115, the number of active elements decreases from 132 to 102. This indicates that the DRL model is effectively shutting down elements to optimize energy efficiency. So, with our proposed method, we can shut down almost 30% of elements, thus increasing the overall energy efficiency for the entire system. Fig. 4c shows the plot between total data rate vs number of episodes for different μ values. Interestingly, It is found that the total data rate remains almost similar for values of μ equals zero and 115. When the μ value is zero, the objective of the system is to maximize the data rates without considering energy efficiency. For the non-zero value of μ , the objective of the system is to optimize energy consumption by penalizing the presence of active redundant elements. Since the two extreme cases of μ value in our scenario (for μ value equals zero and 115), achieve almost similar data rates, this indicates that our DRL model can efficiently balance the trade-off between data rate maximization and energy efficiency for static user scenarios.

B. Impact of mobility on our proposed approach

We now explore the impact of mobility on our method. We specifically focus on a mobility model called ‘‘random waypoint’’ (rwp) [39]. The advantage of rwp lies in its simplicity, wide availability, and unrestricted mobility patterns [39]. In this model, the entity’s movement is characterized by random changes in position and orientation. The UEs move in a square area of 100m² with an average speed of 1m per time step, and at the start of each episode, UE positions are randomly initialized [16]. As the users move, channel conditions become dynamic and lead to time-varying (recall 13, 14, and 15). Here, we consider the scenario of

$N^h = N^v = 12$ STAR-RIS elements. Data rate vs number of episodes for the mobility scenario has been plotted in Fig. 5a. It can be observed that even though our channels are dynamically changing, we still achieve consistent data rates for all users.

Fig. 5b illustrates the plot between the total number of elements active for different μ values and the number of episodes. In this, we examine the cases of μ equal to 0.1 and 115. Due to user mobility, the number of elements allocated to users changes over time. When the μ value is 0.1, an average of 129 elements are actively serving the users. On the other hand, when the μ value is 115, the average number of active elements decreases to 112. From this, we can conclude that the DRL model is effectively shutting down elements even in dynamic user scenarios to optimize energy efficiency. So, with our proposed model, we can shut down almost 22% of elements on average, thus increasing the overall energy efficiency for the entire system. Fig. 5c shows the plot between total data rate vs. number of episodes for μ values equal to zero and 115. It can be observed that even in a dynamic user scenario, the total data rate remains almost similar for $\mu = 0$ and $\mu = 115$ cases because the DRL agent learns to deactivate the excess STAR-RIS elements without any degradation in data rates. Thus, over multiple episodes, the DRL agent learns to adaptively adjust the number of active elements, ensuring efficient resource utilization while maintaining the overall system performance. Our proposed model effectively utilizes DRL to ensure nearly fair rates to all the users across the transmission and reflection spaces while ensuring energy efficiency for the STAR-RIS system.

C. Computational requirement of the proposed algorithm

In our simulations, we have considered three users in the transmission space and three users in the reflection space. Recall that (cf. Section III) to address the huge action space involving STAR-RIS phase shift and subsurface assignment variable, we consider a two-part neural network, with a feed-forward FE and two SNs. At time t , the FE processes the state $\mathbf{u}_0 = \mathbf{s}^{\{t\}}$, with dimension $6 + 2N$. The first entry corresponds to observed SINR values (resulting SINR at the users in both transmission ($\gamma_t^{\{t-1\}}$) and reflection spaces ($\gamma_r^{\{t-1\}}$)) at the time $(t-1)$. Next $2N$ entries correspond to the phase shift and subsurface assignment variable of STAR-RIS, respectively. Assume that each layer of two-layer FE has T neurons. The total floating point operations performed at the FE is $2((6 + 2N)T + T^2)$. The floating point operations for the first and second SN is $2TN$.

V. CONCLUSION

This work lays the foundation for an energy-efficient, fair STAR-RIS system for multiple mobile users. We formulated a novel optimization problem that optimizes both the subsurfaces to be assigned to different users and their corresponding phase shift to give users nearly equal (fair) rates and be energy efficient. The DRL algorithm predicts the STAR-RIS phase shifts and subsurface assignment variable for fair data rates across the users. We first consider the effect

of equal and unequal partitioning of elements of STAR-RIS by DRL optimization. Our results show that, as compared to equal partitioning, the overall data rate increases by an amount of 21% in the static user scenario. The learnable subsurface assignment variable helps us to dynamically allocate the elements even when the users move to get fair data rates across the users based on their location. Further, by using a regularized penalty term for the DRL agent, we can selectively deactivate excess STAR-RIS elements to enhance the energy efficiency of the entire system. Our simulation results indicate that, on average, we can deactivate 30% of STAR-RIS elements in static user scenarios and 22% of STAR-RIS elements in dynamic user scenarios without any loss in performance.

REFERENCES

- [1] E. Basar, M. Di Renzo, J. De Rosny, M. Debbah, M.-S. Alouini, and R. Zhang, "Wireless communications through reconfigurable intelligent surfaces," *IEEE Access*, vol. 7, pp. 116 753–116 773, 2019.
- [2] Y. Liu, X. Mu, J. Xu, R. Schober, Y. Hao, H. V. Poor, and L. Hanzo, "STAR: Simultaneous transmission and reflection for 360° coverage by intelligent surfaces," *IEEE Wireless Commun.*, vol. 28, no. 6, pp. 102–109, 2021.
- [3] X. Mu, Y. Liu, L. Guo, J. Lin, and R. Schober, "Simultaneously transmitting and reflecting (STAR) RIS aided wireless communications," *IEEE Trans. Wireless Commun.*, vol. 21, no. 5, pp. 3083–3098, 2021.
- [4] J. Xu, Y. Liu, X. Mu, R. Schober, and H. V. Poor, "STAR-RISs: A correlated T&R phase-shift model and practical phase-shift configuration strategies," *IEEE J. Sel. Top. Signal Process.*, vol. 16, no. 5, pp. 1097–1111, 2022.
- [5] C. Wu, C. You, Y. Liu, S. Han, and M. D. Renzo, "Two-timescale design for STAR-RIS-aided NOMA systems," *IEEE Trans. Commun.*, vol. 72, no. 1, pp. 585–600, 2024.
- [6] J.-C. Chen, "Energy-efficient hybrid beamforming design for intelligent reflecting surface-assisted mmWave massive MU-MISO systems," *IEEE Trans. Green Commun. Netw.*, vol. 8, no. 1, pp. 330–344, 2024.
- [7] F. Fang, B. Wu, S. Fu, Z. Ding, and X. Wang, "Energy-efficient design of STAR-RIS aided MIMO-NOMA networks," *IEEE Trans. Commun.*, vol. 71, no. 1, pp. 498–511, 2023.
- [8] Y. Guo, F. Fang, D. Cai, and Z. Ding, "Energy-efficient design for a NOMA assisted STAR-RIS network with deep reinforcement learning," *IEEE Trans. Veh. Technol.*, vol. 72, no. 4, pp. 5424–5428, 2023.
- [9] P. Guan, Y. Wang, H. Yu, and Y. Zhao, "Energy efficiency maximisation for STAR-RIS assisted full-duplex communications," *IET Commun.*, vol. 17, no. 5, pp. 603–613, 2023.
- [10] Q. Zhang, Y. Zhao, H. Li, S. Hou, and Z. Song, "Joint optimization of STAR-RIS assisted UAV communication systems," *IEEE Wireless Commun. Lett.*, vol. 11, no. 11, pp. 2390–2394, 2022.
- [11] M. Aldababsa, A. Khaleel, and E. Basar, "STAR-RIS-NOMA networks: An error performance perspective," *IEEE Commun. Lett.*, vol. 26, no. 8, pp. 1784–1788, 2022.
- [12] J. Zhao, Y. Zhu, X. Mu, K. Cai, Y. Liu, and L. Hanzo, "Simultaneously transmitting and reflecting reconfigurable intelligent surface (STAR-RIS) assisted UAV communications," *IEEE J. Sel. Areas Commun.*, vol. 40, no. 10, pp. 3041–3056, 2022.
- [13] Q. Wu and R. Zhang, "Intelligent reflecting surface enhanced wireless network via joint active and passive beamforming," *IEEE Trans. Wireless Commun.*, vol. 18, no. 11, pp. 5394–5409, 2019.
- [14] G. Pan, J. Ye, J. An, and M.-S. Alouini, "Full-duplex enabled intelligent reflecting surface systems: Opportunities and challenges," *IEEE Wireless Commun.*, vol. 28, no. 3, pp. 122–129, 2021.
- [15] P. P. Perera, V. G. Warnasooriya, D. Kudathanthirige, and H. A. Suraweera, "Sum rate maximization in STAR-RIS assisted full-duplex communication systems," in *Proc. 2022 IEEE International Conference on Communications (ICC)*, 2022, pp. 3281–3286.
- [16] N. Nayak, S. Kalyani, and H. A. Suraweera, "A DRL approach for RIS-assisted full-duplex UL and DL transmission: Beamforming, phase shift and power optimization," *IEEE Trans. Wireless Commun.*, 2024.
- [17] Z. Ma, Q. Zhao, B. Yan, and J. Zhang, "Deep reinforcement learning enabled joint deployment and beamforming in STAR-RIS assisted networks," *arXiv preprint arXiv:2309.03520*, 2023.
- [18] L. Wang, B. Ai, Y. Niu, Z. Zhong, Z. Han, and N. Wang, "Joint reliability optimization and beamforming design for STAR-RIS-aided multi-user MISO URLLC systems," *IEEE Trans. Veh. Technol.*, pp. 1–15, 2024.
- [19] X. Gao, W. Yi, Y. Liu, J. Zhang, and P. Zhang, "DRL enabled coverage and capacity optimization in STAR-RIS-assisted networks," *IEEE Trans. Commun.*, no. 11, pp. 6616–6632, 2023.
- [20] Y. Hu, K. Kang, H. Zhu, X. Luo, and H. Qian, "Serving mobile users in intelligent reflecting surface assisted massive MIMO System," *IEEE Trans. Veh. Technol.*, vol. 71, no. 6, pp. 6384–6396, 2022.
- [21] Z. Huang, B. Zheng, and R. Zhang, "Transforming fading channel from fast to slow: Irs-assisted high-mobility communication," in *Proc. 2021 IEEE International Conference on Communications (ICC)*, 2021, pp. 1–6.
- [22] M. Ahmed, A. Wahid, S. S. Laique, W. U. Khan, A. Ihsan, F. Xu, S. Chatzinotas, and Z. Han, "A survey on STAR-RIS: Use cases, recent advances, and future research challenges," *IEEE Internet Things J.*, vol. 10, no. 16, pp. 14 689–14 711, 2023.
- [23] Y. Cai, M.-M. Zhao, K. Xu, and R. Zhang, "Intelligent reflecting surface aided full-duplex communication: Passive beamforming and deployment design," *IEEE Trans. Wireless Commun.*, vol. 21, no. 1, pp. 383–397, 2021.
- [24] K. Feng, Q. Wang, X. Li, and C.-K. Wen, "Deep reinforcement learning based intelligent reflecting surface optimization for MISO communication systems," *IEEE Wireless Commun. Lett.*, vol. 9, no. 5, pp. 745–749, 2020.
- [25] K. Wang, C.-T. Lam, and B. K. Ng, "RIS-assisted high-speed communications with time-varying distance-dependent Rician channels," *Applied Sciences*, vol. 12, no. 22, p. 11857, 2022.
- [26] S. Zhang, S. Bao, K. Chi, K. Yu, and S. Mumtaz, "DRL-based computation rate maximization for wireless powered multi-AP edge computing," *IEEE Trans. Commun.*, 2023.
- [27] T. Zhang, P. Ren, D. Xu, and Z. Ren, "RIS subarray optimization with reinforcement learning for green symbiotic communications in Internet of Things," *IEEE Internet Things J.*, vol. 10, no. 22, pp. 19 454–19 465, 2023.
- [28] P. S. Aung, L. X. Nguyen, Y. K. Tun, Z. Han, and C. S. Hong, "Aerial STAR-RIS empowered MEC: A DRL approach for energy minimization," *IEEE Wireless Commun. Lett.*, vol. 13, no. 5, pp. 1409–1413, 2024.
- [29] K. Feng, Q. Wang, X. Li, and C.-K. Wen, "Deep reinforcement learning based intelligent reflecting surface optimization for MISO communication systems," *IEEE Wireless Commun. Lett.*, vol. 9, no. 5, pp. 745–749, 2020.
- [30] V. Raj, N. Nayak, and S. Kalyani, "Deep reinforcement learning based blind mmWave MIMO beam alignment," *IEEE Trans. Wireless Commun.*, vol. 21, no. 10, pp. 8772–8785, 2022.
- [31] T. P. Lillicrap, J. J. Hunt, A. Pritzel, N. Heess, T. Erez, Y. Tassa, D. Silver, and D. Wierstra, "Continuous control with deep reinforcement learning," *arXiv preprint arXiv:1509.02971*, 2015.
- [32] V. Mnih, K. Kavukcuoglu, D. Silver, A. Graves, I. Antonoglou, D. Wierstra, and M. Riedmiller, "Playing atari with deep reinforcement learning," *arXiv preprint arXiv:1312.5602*, 2013.
- [33] W. Ni, Y. Liu, Y. C. Eldar, Z. Yang, and H. Tian, "STAR-RIS integrated nonorthogonal multiple access and over-the-air federated learning: Framework, analysis, and optimization," *IEEE Internet Things J.*, vol. 9, no. 18, pp. 17 136–17 156, 2022.
- [34] M. Umer, M. A. Mohsin, S. A. Hassan, H. Jung, and H. Pervaiz, "Performance analysis of STAR-RIS enhanced CoMP-NOMA multi-cell networks," in *Proc. 2023 IEEE Globecom Workshops (GC Wkshps)*, 2023, pp. 2000–2005.
- [35] A. Taha, Y. Zhang, F. B. Mismar, and A. Alkhateeb, "Deep reinforcement learning for intelligent reflecting surfaces: Towards standalone operation," in *Proc. IEEE 21st international workshop on signal processing advances in wireless communications (SPAWC 2020)*, 2020, pp. 1–5.
- [36] Z. Peng, Z. Zhang, C. Pan, L. Li, and A. L. Swindlehurst, "Multiuser full-duplex two-way communications via intelligent reflecting surface," *IEEE Trans. Signal Process.*, vol. 69, pp. 837–851, 2021.
- [37] N. Docomo *et al.*, "5G channel model for bands up to 100 GHz," Tech. Report, Oct, Tech. Rep., 2016.
- [38] T. S. Rappaport, *Wireless communications: principles and practice*. Cambridge University Press, 2024.
- [39] D. B. Johnson and D. A. Maltz, "Dynamic source routing in ad hoc wireless networks," *Mobile Computing*, pp. 153–181, 1996.